Mon. Not. R. astr. Soc. (1981) **196**, 1067–1086

A new method for making maps with unstable radio interferometers

T. J. Cornwell* and P. N. Wilkinson *University of Manchester, Nuffield Radio Astronomy Laboratories, Jodrell Bank, Macclesfield, Cheshire SK11 9DL*

Received 1981 February 13; in original form 1980 November 5

Summary. We present a new method for making 'hybrid' maps using data from unstable interferometers. Our approach is based on correcting errors occurring at individual telescopes, and is more general than previous ones in that it allows for different degrees of instability at each telescope as well as for varying signal-to-noise ratios in the visibility data on each baseline. The method was developed, and will be used, for the analysis of the data from the Jodrell Bank Multi-Telescope Radio-Linked Interferometer (MTRLI). We show the results of tests on simulated data to indicate the quality of maps which can be made with the MTRLI using the new method, and present a hybrid map of the quasar 3C 309.1 made from actual MTRLI data at 1666 MHz.

1 Introduction

In the past few years, considerable attention has been paid to the problem of map-making with radio interferometers which do not preserve accurately the phase of the interference fringes. Much of the impetus for these developments has come from VLBI where the phase problem is most acute, and considerable success has been achieved by the use of the so-called 'closure' phase in networks containing three or more telescopes. This observable was first used in the context of VLBI by Rogers *et al.* (1974). As a result of subsequent developments by Fort & Yee (1976), Readhead & Wilkinson (1978) and Cotton (1979), reliable maps, whose quality approaches that from conventional interferometers, can now be made routinely in the face of total ignorance of the phase on individual baselines. More recently Readhead *et al.* (1980) have demonstrated that, using the so-called 'closure' amplitudes, useful maps can also be made even if there are gross errors in the fringe amplitudes. Maps made from imperfect data using these unconventional techniques have come to be known as 'hybrid' maps (following Baldwin & Warner 1976).

In this paper we describe a new and more general method of making hybrid maps which takes signal-to-noise ratios into account and allows for the fact that there may be different levels of phase and amplitude instability at each telescope. The telescope-related logic of our method means that it is also easier to apply to data from arrays of many telescopes than the

*Present address: NRAO, VLA Program, Socorro, New Mexico.

earlier, baseline-related, ones. We give a practical example of the use of our method by showing a hybrid map of 3C 309.1 made with the Jodrell Bank Multi-Telescope Radio-Linked Interferometer (MTRLI) (Davies, Anderson & Morison 1980) at 1666 MHz. It is anticipated that the majority of maps produced from the MTRLI will in fact be hybrid maps, and this paper will serve to describe the method used to produce them. It is, of course, equally applicable to data from any interferometer network.

2 Background

2.1 CLOSURE RELATIONS

In the absence of noise, and assuming that perfect correlators are used, the only sources of error in the measurements of the complex visibility function of a radio source made with an interferometer array are associated with the individual telescopes. The fringe amplitudes are corrupted by such effects as receiver sensitivity drifts, telescope pointing errors and gain-elevation dependence, while the phases are corrupted by changes in relative delay due to various drifts in the electronics, atmospheric path-length changes and imperfect knowledge of the source position and interferometer geometry. Thus, in an N-telescope array at any one time, there are only N complex errors associated with the $N(N-1)/2$ independent complex observables, the fringe amplitude and phase on each baseline. There are therefore $[N(N-1)/2]-N$ complex quantities which are uncorrupted by telescope effects; these are the so-called 'closure' quantities. Jennison (1953, 1958) was the first to recognize this by introducing the concept of the closure phase, a linear combination of observed phases around a closed loop of baselines formed from three or more telescopes. Somewhat later Twiss, Carter & Little (1960) introduced an analogous quantity, the closure amplitude, formed from the ratios of observed fringe amplitudes from a network of at least four telescopes.

To derive these closure quantities, we need to define a relationship between the observed and true complex visibilities (V_{jk} and $\hat{V}_{jk}$ respectively) on the single interferometer baseline between telescopes j and k. This arises from the definition of the complex correlation coefficient of the electric fields at the two telescopes (see e.g. Fomalont 1973) and the assumptions described above. The relation can be written as

$$V_{jk} = \hat{V}_{jk}\,(1+a_j)\,(1+a_k)\exp i(\phi_j-\phi_k)+\epsilon_{jk}, \tag{1}$$

where a_j, ϕ_j are the amplitude and phase errors at the jth telescope, and ϵ_{jk} is the complex error due to thermal noise.

The closure relations arise naturally by taking ratios of equations such as these (see also Readhead *et al.* 1980). The simplest example of a closure phase is

$$C_{jkl} = \theta_{jk}+\theta_{kl}+\theta_{lj}, \tag{2}$$

where

$$\theta_{jk} = \arg(V_{jk}). \tag{3}$$

Ignoring the noise terms, this is equal to the same sum of the *true* visibility phases. The simplest closure amplitudes are of the form

$$A_{jklm} = \frac{|V_{jk}|\,|V_{lm}|}{|V_{jl}|\,|V_{km}|}. \tag{4}$$

Closure-amplitude information is only available from networks comprising at least four telescopes, but as in Jennison's original application, a closure phase can be formed from three telescopes. This is because the measured interferometer phase is only the *difference* between the phases of signals in each interferometer arm, the absolute phase in each arm has no significance and consequently we are free to assign an arbitrary phase – most conveniently zero – to one telescope and refer all other phases to this. In an N telescope network therefore there are $N-1$ rather than N unknown telescope phase errors. These closure quantities are completely independent of source strength and position, and hence maps made using only them as constraints have arbitrary position offsets and flux density scales.

Before leaving this discussion we should note that there *is* one telescope-related effect which can corrupt even the closure quantities. If the amplitude and phase response of the defining passbands in each interferometer arm are not identical, then the observed complex visibility of an interferometer cannot be factorized simpy as in equation (1). This problem has been discussed by Thompson (1980) who has shown that it affects the closure amplitudes more severely than the closure phases.

2.2 THE NEED FOR A NEW HYBRID MAPPING METHOD

As we have mentioned, there are several accounts in the literature of ways in which the measured amplitudes and the closure phases can be used to constrain maps of the radio brightness distribution. Nearly all of these methods make corrections to the phases *on individual baselines* consistent with the closure phases. It is useful to outline the best known and most widely used of these, due to Readhead & Wilkinson (1978) (hereafter RW), in order to understand why we felt it worthwhile to develop a new method to analyse MTRLI data.

For an N-telescope network, RW force the visibility phases on $N-1$ baselines to have the values predicted by a trial map of the brightness distribution. The phases on the other baselines are chosen to satisfy the measured closure phases. This whole set of constructed visibility phases is then used within the observed amplitudes to form a new trial map of the brightness distribution via the CLEAN process (Högbom 1974). Visibility phases on $N-1$ baselines are again predicted from this trial map and the process is then repeated until convergence is attained. The main agent responsible for convergence is CLEAN, which is used to eliminate what are thought to be spurious components in the trial maps at each iteration. Recently Readhead *et al.* (1980) have extended this algorithm to utilize closure amplitudes in an analogous manner, calculating N amplitudes from the trial map at each iteration.

This straightforward approach works well on data from only a few telescopes, in which all baselines have equally poor phase-stability and reasonable signal-to-noise ratios; this is the situation with much present-day VLBI data. However, when dealing with data from a partially stable interferometer network, such as the MTRLI will be at certain frequencies, notice should be taken of the visibility phases themselves. In this case RW's method would not make optimum use of the available information, for in utilizing only the closure phases no allowance is made for the fact that some baselines may be more phase-stable than others. RW also do not allow for the different signal-to-noise ratios on the separate baselines. Thus while the method may 'converge' to give an acceptable map, it will not in general yield the map with the highest possible dynamic range.

Schwab (1980), considering the problem of improving VLA maps, has gone some way towards developing a more general method which is based on a consideration of the errors at *individual telescopes* and which avoids some of the shortcomings of the RW method. His approach is formally equivalent to using the closure quantities explicitly, but is a more logical way to tackle the problem. In Schwab's method, the telescope-related amplitude and

phase errors are adjusted iteratively to minimize the weighted sum of squares

$$S = \sum_{\substack{j,\ k \\ j<k}} |V_{jk} - \hat{V}_{jk}\,(1+a_j)\,(1+a_k)\exp(\phi_j - \phi_k)|^2\, w_{jk}. \tag{5}$$

The w_{jk}s are weighting factors which can be chosen to favour baselines of good signal-to-noise ratio. As in the RW method a trial map is used to give estimates of $\hat{V}_{jk}$. Having obtained new estimates of the a_j, ϕ_j, these are used to correct the observed visibilities, V_{jk}, on each baseline. A new trial map is then made from these corrected visibilities by means of CLEAN.

We also have developed a method along these lines but which is rather more general than Schwab's. We now go on to show how, by explicitly accepting the fact that errors originate at individual telescopes, we are led naturally to a concise formulation of the general problem.

3 The new method

3.1 THE THEORY

Given estimates of the true visibilities $\hat{V}_{jk}$ on each baseline, obtained from the trial map, the problem reduces to that of finding optimum estimates of the amplitude and phase errors a_j, ϕ_j which have occurred at each telescope to produce the observed corrupted data.

If the a_j, ϕ_j errors are regarded as random variables whose probability density functions (pdf) are known, the joint pdf of all the errors at any one time, including receiver noise, can be written as

$$P([a_j], [\phi_j], [\epsilon_{jk}]) = P([a_j])\,P([\phi_j])\,P([\epsilon_{jk}]), \tag{6}$$

since the errors arise from different physical processes and are therefore independent. Here the square brackets denote a set of variables. Any decision made about these errors must take into account their likelihood. For example, we could arbitrarily assign values to the amplitude and phase errors, but then the receiver noise terms, constrained by equation (1), may be completely unlikely. However, equation (6) allows us to make sensible estimates of all the errors, namely the most probable set obeying equation (1). Formally we wish to maximize the joint pdf with respect to the errors, subject to the relationship between the thermal noise and the a_j, ϕ_j errors expressed in equation (1). The form of the pdf for the receiver noise can be assumed to be a two-dimensional Gaussian, thus

$$P(\epsilon_{jk}) = \frac{1}{2\pi\sigma_{jk}^2}\exp(-|\epsilon_{jk}|^2/2\sigma_{jk}^2), \tag{7}$$

where σ_{jk}^2 is the variance of the real or imaginary part of the noise vector ϵ_{jk}. For any one integration period, the pdf of the set of receiver noises, $P([\epsilon_{jk}])$, is a product of terms such as these, one for each baseline. If, as is usual, we do not know *a priori* the pdf for the a_j, ϕ_j errors, we have to assign forms to them arbitrarily in order to proceed; in practice it seems that the exact form is not important and for convenience we have assumed that both are one-dimensional Gaussians. Explicitly, writing the amplitude and phase variances as σ_{a_j}, σ_{ϕ_j} and assuming both the errors to have zero mean, the pdf may be expressed as

$$P(a_j) = \frac{1}{(2\pi\sigma_{a_j}^2)^{1/2}}\exp(-a_j^2/2\sigma_{a_j}^2) \tag{8}$$

and

$$P(\phi_j) = \frac{1}{(2\pi\sigma_{\phi_j}^2)^{1/2}}\exp(-\phi_j^2/2\sigma_{\phi_j}^2). \tag{9}$$

Again, the pdf for the sets for any one integration period are formed from the products of such terms, one for each telescope. Note that we are making the simplifying assumption that all the error statistics are stationary. Note also that because, as described in Section 2.1, an interferometer can only measure phase differences, one can choose the phase error of one telescope to be zero. Consequently for that reference telescope $\sigma_{\phi_{\text{ref}}} \equiv 0$.

Now the constraints implied by equation (1) can be included by substituting for ϵ_{jk} in equation (6). This removes one subset of independent variables from the joint pdf, and restricts us to choosing only the a_j and ϕ_js to maximize the joint pdf. Without loss of generality we instead maximize the logarithm of the joint pdf, and thus maximize

$$2 \ln \{P([a_j], [\phi_j], [\epsilon_{jk}])\} = -\sum_j a_j^2/\sigma_{a_j}^2 - \sum_j \phi_j^2/\sigma_{\phi_j}^2 - \sum_{\substack{j,\,k \\ j>k}} \frac{|V_{jk} - \hat{V}_{jk}\,(1+a_j)\,(1+a_k)\exp i(\phi_j - \phi_k)|^2}{\sigma_{jk}^2} + \text{const.} \tag{10}$$

If the uncertainties in the a_j, ϕ_js are great, i.e. σ_{a_j} and σ_{ϕ_j} are very large, the first two terms on the right-hand side can be neglected. In this case the problem reduces to that considered by Schwab (1980).

The maximization can be performed numerically as Schwab does but, in order to treat the problem analytically, we consider the amplitude and phase errors separately. Consider first the phase errors and ignore any amplitude errors, i.e. set the a_js to zero. Differentiating equation (10) with respect to ϕ_j and setting to zero yields the set of non-linear equations

$$\sum_{k \neq j} \frac{|V_{jk}|\,|\hat{V}_{jk}|}{\sigma_{jk}^2} \sin\,(\theta_{jk} - \hat{\theta}_{jk} - \phi_j + \phi_k) = \frac{\phi_j}{\sigma_{\phi_j}^2}. \tag{11}$$

These equations can be made more tractable by linearizing them using the small-angle approximation for sine. The resulting linear equations

$$\sum_{k \neq j} \frac{|V_{jk}|\,|\hat{V}_{jk}|}{\sigma_{jk}^2} (\theta_{jk} - \hat{\theta}_{jk} - \phi_j + \phi_k) = \frac{\phi_j}{\sigma_{\phi_j}^2} \tag{12}$$

can now be solved by matrix inversion, and so this simplification considerably increases the speed of the algorithm.

We can gain greater physical insight into these equations by deriving them heuristically, if not exactly, in the following stepwise fashion. Consider first the phase of equation (1) and ignore the noise term. We then have

$$\theta_{jk} - \hat{\theta}_{jk} - \phi_j + \phi_k = 0. \tag{13}$$

There are $N(N-1)/2$ of these equations which we want to solve for the N σ_js. For the jth telescope we have $(N-1)$ equations which can be summed to yield

$$(N-1)\,\phi_j = \sum_{k \neq j} \phi_k + \sum_{k \neq j} (\theta_{jk} - \hat{\theta}_{jk}) \tag{14}$$

but, as described in Section 2.1, one of the telescopes can be used as a reference and its

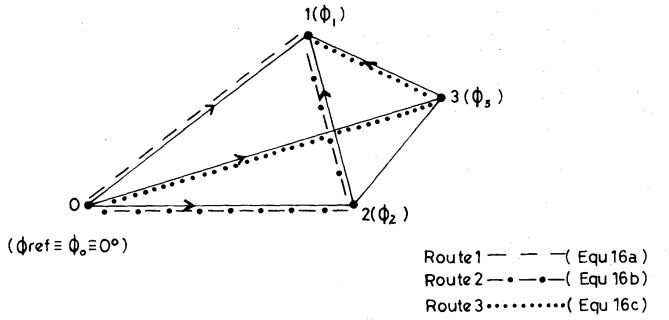

Figure 1. A four-telescope array illustrating the three independent ways of estimating the phase error at telescope 1.

phase error ϕ_{ref} set to zero. We can then rearrange this equation to yield:

$$\phi_j = \frac{1}{N-1}\left[\sum_{k \neq j}(\theta_{jk} - \hat{\theta}_{jk}) - \sum_{\substack{k \neq \text{ref} \\ k \neq j}}(\theta_{\text{ref},k} - \hat{\theta}_{\text{ref},k})\right]. \tag{15}$$

Specifically, for the four-telescope array shown in Fig. 1, there are three independent ways of deriving the phase error at any given telescope. For example, for ϕ_1 we have:

$$\phi_1 = (\theta_{10} - \hat{\theta}_{10}), \tag{16a}$$

$$\phi_1 = (\theta_{12} - \hat{\theta}_{12}) + \phi_2 = (\theta_{12} - \hat{\theta}_{12}) - (\theta_{02} - \hat{\theta}_{02}), \tag{16b}$$

$$\phi_1 = (\theta_{13} - \hat{\theta}_{13}) + \phi_3 = (\theta_{13} - \hat{\theta}_{13}) - (\theta_{03} - \hat{\theta}_{03}). \tag{16c}$$

However, as the $\hat{\theta}_{jk}$s are only *estimates* of the true phases from a trial map, in general the best estimate of ϕ_1 is an average of the three values. This then corresponds to a particular case of equations (15). So far we have used equation (13) with no regard to the signal-to-noise ratio. In summing such equations we should weight them by the inverse of the variance of the phase error due to noise, i.e. by $|\hat{V}_{jk}/\sigma_{jk}|^2$. Thus this simple derivation yields the equations:

$$\sum_{k \neq j} \frac{|\hat{V}_{jk}|^2}{\sigma_{jk}^2}(\theta_{jk} - \hat{\theta}_{jk} - \phi_j + \phi_k) = 0. \tag{17}$$

No prior knowledge of the likely distribution of phase errors at each telescope has been assumed here. In fact it is implicit that they are all equally probable between ±180°. This corresponds to the specific case of a phase-unstable system. In many cases, however, we do have some confidence in the absolute phases. For example, the expected phase deviations may be small for telescopes close to the reference telescope so that these baselines are more phase-stable than the longer baselines. This is explicitly recognized in the more generalized formulation considered above, and this results in the extra term on the right-hand side of equation (11) for the special case of a Gaussian distribution of phase errors.

One practical difficulty arises from linearizing the phase equations. Consider, for example, equations (15). Since the phases are known modulo 360°, errors of integer multiples (n) of $360°/(N-1)$ can occur in the solution for ϕ_j. To avoid this problem one must ensure that the phase errors $(\theta_{jk} - \hat{\theta}_{jk})$ around any closed loop of baselines sum to zero within the noise and not to $n.360°$. In fact this is the only place where closure phases are explicitly calculated in the method.

Having considered the phase errors we can now treat the amplitude errors in an analogous fashion. Returning to equation (10), make the approximation that $(1+a_j)(1+a_k) \simeq 1+a_j+a_k$. This is valid if the a_js are close to zero. Now, differentiating equation (10) with respect to a_j, setting to zero, and ignoring phase errors, we obtain directly a set of linear equations

$$\sum_{k \neq j} \left[\frac{\mathrm{Re}(V_{jk}\hat{V}_{jk}^*)}{\sigma_{jk}^2} - \frac{|\hat{V}_{jk}|^2}{\sigma_{jk}^2}(1+a_j+a_k) \right] = \frac{a_j}{\sigma_{a_j}^2}. \tag{18}$$

But since we are now assuming that there are no phase errors present (or that they have been already corrected), we can replace Re $(V_{jk}\hat{V}_{jk}^*)$ by $|V_{jk}| \cdot |\hat{V}_{jk}|$ and thus obtain:

$$\sum_{k \neq j} \frac{|\hat{V}_{jk}|^2}{\sigma_{jk}^2} \left[\frac{|V_{jk}|}{|\hat{V}_{jk}|} - (1+a_j+a_k) \right] = \frac{a_j}{\sigma_{a_j}^2}. \tag{19}$$

Again the essential features of these equations can be understood simply. Returning to equation (1), and assuming no phase errors and no receiver noise, we obtain

$$|V_{jk}| - (1+a_j)(1+a_k)|\hat{V}_{jk}| = 0, \tag{20}$$

or, using the small error approximation,

$$\frac{|V_{jk}|}{|\hat{V}_{jk}|} - (1+a_j+a_k) = 0. \tag{21}$$

Again we should sum such equations weighting by the inverse of the variance of the amplitude errors due to finite signal-to-noise ratio, i.e. by $|\hat{V}_{jk}/\sigma_{jk}|^2$. The right-hand side of equation (19) allows for the prior knowledge of the amplitude stability of the separate telescopes.

3.2 PRACTICAL DETAILS

We have developed a FORTRAN program (CORTEL; for CORrect TELescopes) to make these telescope-related corrections to the observed amplitudes and phases. This is used in an iterative procedure, similar to that employed by RW, to improve a trial map of the source. Unlike RW's method, when using CORTEL it is not necessary to store any closure data in the computer, since all the manipulations are performed on the complex visibilities themselves. This means that the storage requirements are the same as for conventional interferometry. A flow diagram of the procedure is shown in Fig. 2.

First a trial map is used to calculate $|\hat{V}_{jk}|$ and $\hat{\theta}_{jk}$ for all the observed data points via a direct Fourier transform. The program then takes the data from all available baselines for the first integration period and calculates the phase and the amplitude errors by matrix solution of equations (12) and (19). These matrix equations are then solved in turn for all the individual integration periods in the run, treating each period separately. Missing data are simply accommodated by leaving out the relevant term in the summations in the equations. Our formulation ensures that, if there are data on fewer baselines than there are errors to be calculated, then the visibilities on some baselines will be those obtained directly from the trial map. The observed data are then corrected and passed to a conventional mapping program, in our case CLEAN, to produce a new trial map. The discussion given by RW about the details of CLEAN and its role in convergence is both relevant and adequate for our present purpose. The whole process is then repeated, but, in subsequent iterations, corrections can

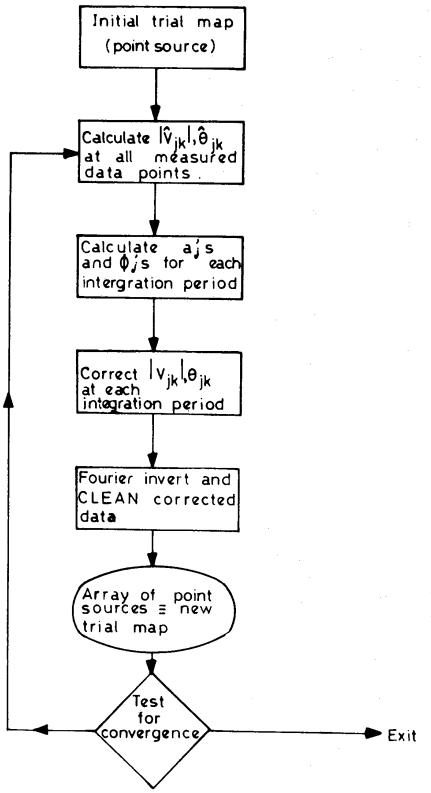

Figure 2. A flow diagram of the method.

be applied to the modified data from the previous iteration. This means that the a_j, ϕ_j corrections tend to zero as the process converges, and hence the approximations inherent in linearizing the problem become increasingly valid.

The ultimate test of convergence is that the Fourier transform of the delta functions output from CLEAN fits the corrected amplitudes and phases from which they were derived. Since the program only makes telescope-related adjustments, this is exactly equivalent to requiring that the transform of the delta functions fits the closure amplitudes and phases.

The program is more general than previous ones in that *a priori* knowledge of the different levels of amplitude and phase errors on each telescope can be utilized. These are assumed to be constant throughout the whole observing run and are set by the σ_{a_j} and σ_{ϕ_j} parameters. For total ignorance of the phase on each telescope, as in VLBI, σ_{ϕ_j} is set to be very large. Finally there is an option to allow only a constant amplitude-error at each telescope during a whole observing run on a source. This is performed in the program by summing the left-hand side of equation (19) over all integration periods. This option is useful in VLBI applications when absolute amplitude calibration can be difficult but when relative changes in the calibration of each telescope are well understood.

4 Tests of the method

The fact that satisfactory hybrid maps can be made from closure phase and closure-amplitude data has been demonstrated by blind testing (Readhead & Wilkinson 1978; Cotton 1979; Readhead *et al.* 1980). The present method requires little user-intervention and so we considered that further blind tests were unnecessary. In fact, in the tests described below, the only significant user-decision required was to set the overall map-size. No 'windows' smaller than this overall size were used to reject spurious components. These tests were designed to

illustrate not only the capabilities of our method but also of the MTRLI at a representative declination.

Test 1. A simulated data set was formed by Fourier-transforming a model composed of elliptical Gaussians (very similar to that used in test 4 of RW) with a total flux density of 31 Jy. The parameters of the six Gaussian components comprising this model are as follows:

Flux density (Jy)	Vector distance from origin (arcsec)	(degrees)	Major axis (arcsec)	Axial ratio	Position angle of elongation (degrees)
6.0	1.5	−35.0	1.2	1.0	0.0
8.0	4.4	−30.0	2.0	0.7	−80.0
12.0	2.5	140.0	1.8	0.6	−22.0
3.0	4.5	130.0	1.2	1.0	0.0
1.0	3.5	−135.0	0.8	1.0	0.0
1.0	2.5	140.0	0.0	1.0	0.0

The u, v coverage was that which would be obtained using five telescopes of the MTRLI at 408 MHz for a source of declination 50°. This is shown in Fig. 3. For each integration time of three minutes, the data were corrupted by 5 per cent rms amplitude errors and phase errors completely random between ±180°. These errors were added per telescope not per baseline, although receiver noise of 50 mJy rms was added to the data on each baseline at each integration time. The data set was constructed in this way so that its quality would be similar to that of data obtained on the stronger sources in the first observing session of MTRLI at 408 MHz. As we discuss later, these errors do not represent what we think will be typical errors in future MTRLI observations.

Our starting model in this test, and in all those which follow, was a point source. Initially, in this test only, we only corrected the phases and therefore used the 'observed' amplitudes with corrected phases to produce trial maps. As the process converged we then switched on

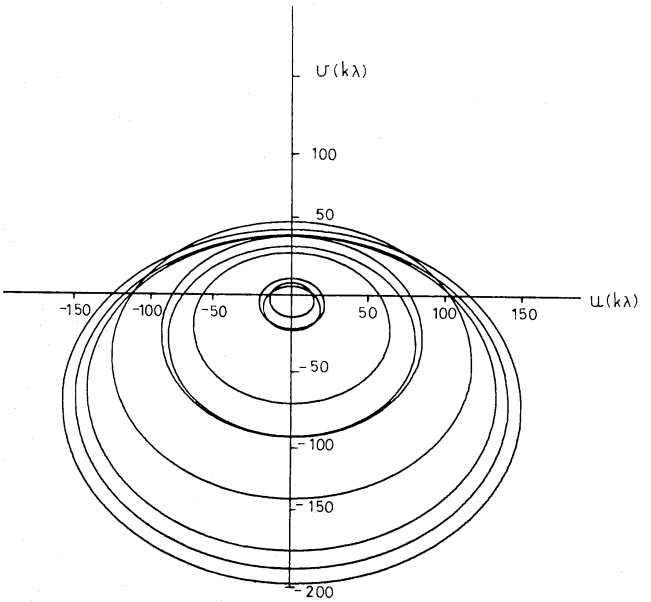

Figure 3. The aperture plane (u, v) coverage assumed in the tests of the CORTEL program. This corresponds to that which would be obtained using five telescopes of the MTRLI at declination 50° and an observing frequency at 408 MHz.

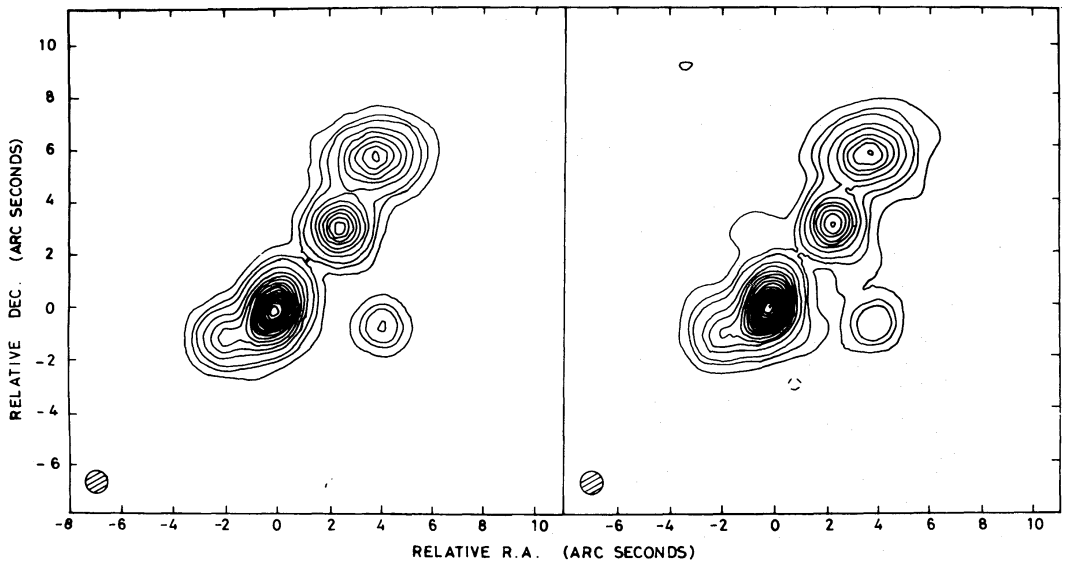

Figure 4. Test 1: a strong source. (a) (left) A map made assuming perfect amplitude- and phase-stability. (b) (right) The hybrid map made from corrupted data. In this and all subsequent tests the restoring beam has FWHM = 0.9 arcsec, corresponding to MTRLI operation at 408 MHz. The contour levels are 1, 3, 5, 10, 15, ..., 95 per cent of the peak brightness. A contour level of 1 per cent corresponds to 50 ± ~3 mJy per clean beam area.

the amplitude correction. The final hybrid map is shown in Fig. 4(b). In Fig. 4(a) we show the map which would be obtained with perfect amplitude and phase stability but still with receiver noise. In both cases we have used a restoring beam of FWHM = 0.9 arcsec. It can be seen from this test that maps reliable at the ~ 2 per cent level can be produced from such data. In Fig. 5 we show fits to the closure phase and amplitude data for the delta functions, produced by the CLEAN process, which are the basis of Fig. 4(b).

Test 2. For this test we used the same data set as in test 1 but with a higher level of receiver noise, 1.5 Jy, for each integration time. The data quality corresponds to that which would

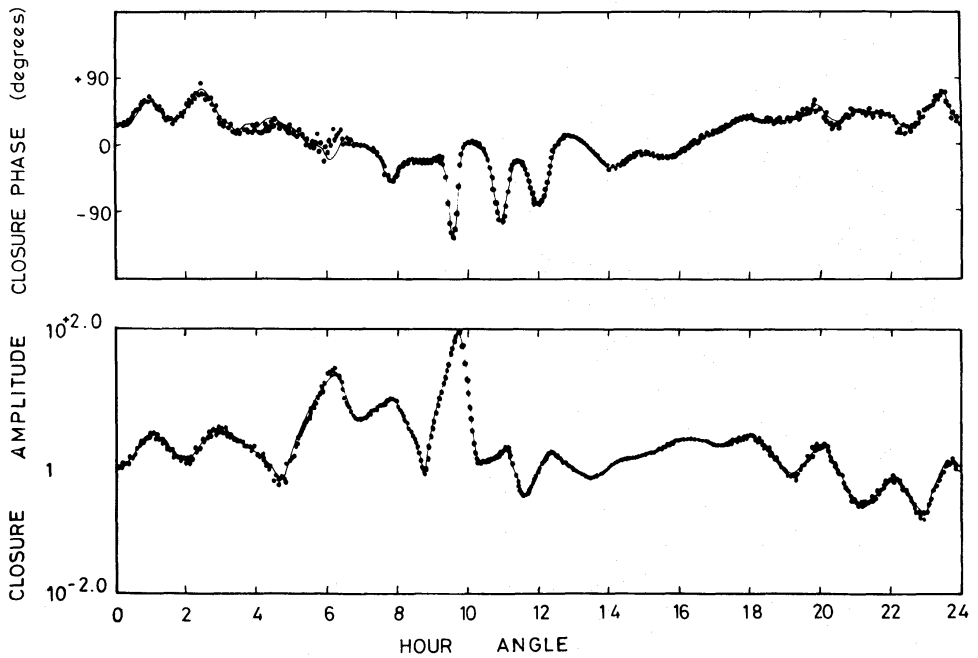

Figure 5. One of the closure phases and one of the closure amplitudes used in test 1. The solid lines were obtained from the Fourier transform of the delta functions comprising Fig. 4.

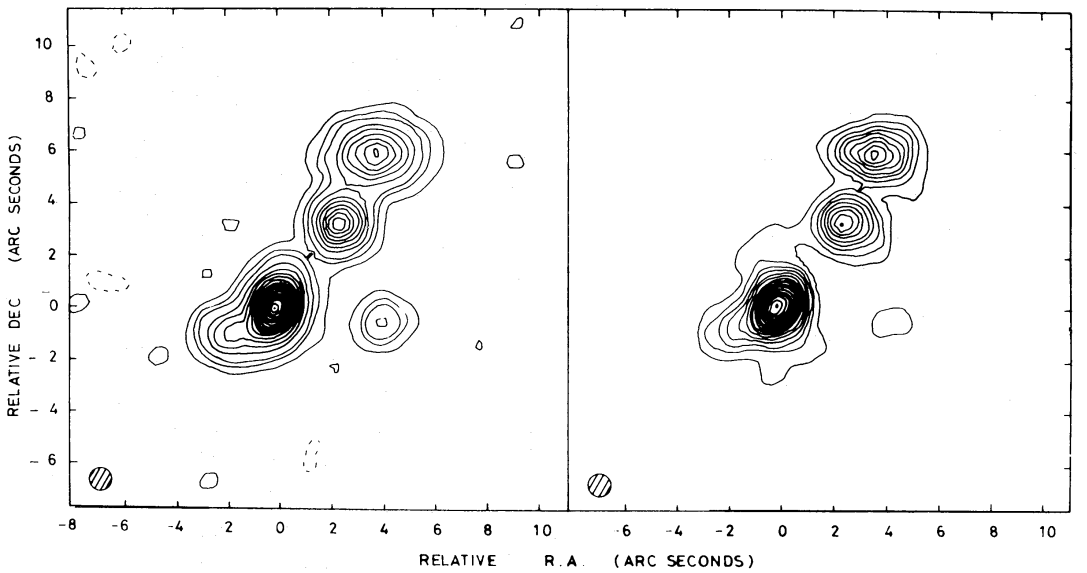

Figure 6. Test 2: a weak source. (a) (left) The map obtained from stable data. The contour levels are 1, 3, 5, 10, . . . , 95 per cent. A 1 per cent contour corresponds to 1.7 mJy per clean beam area. (b) (right) The hybrid map. The contour levels are 5, 10, 15, . . . , 95 per cent. A 1 per cent contour corresponds to 1.7 ± ~0.04 mJy per clean beam area.

have been obtained on a complex, heavily resolved, source of flux density ~1 Jy in the first MTRLI session. The final hybrid map is shown in Fig. 6(b). In Fig. 6(a) we show the map which would have been obtained with perfect amplitude and phase stability but with the higher level of receiver noise. In Fig. 7 we show the fits to one of the closure phases and one of the closure amplitudes for the delta functions which are the basis of Fig. 6(a). The large amount of noise seen on these closure data occurs because for long periods the fringe visibility drops to about the noise level on the longer baselines. Note that the bottom contour in

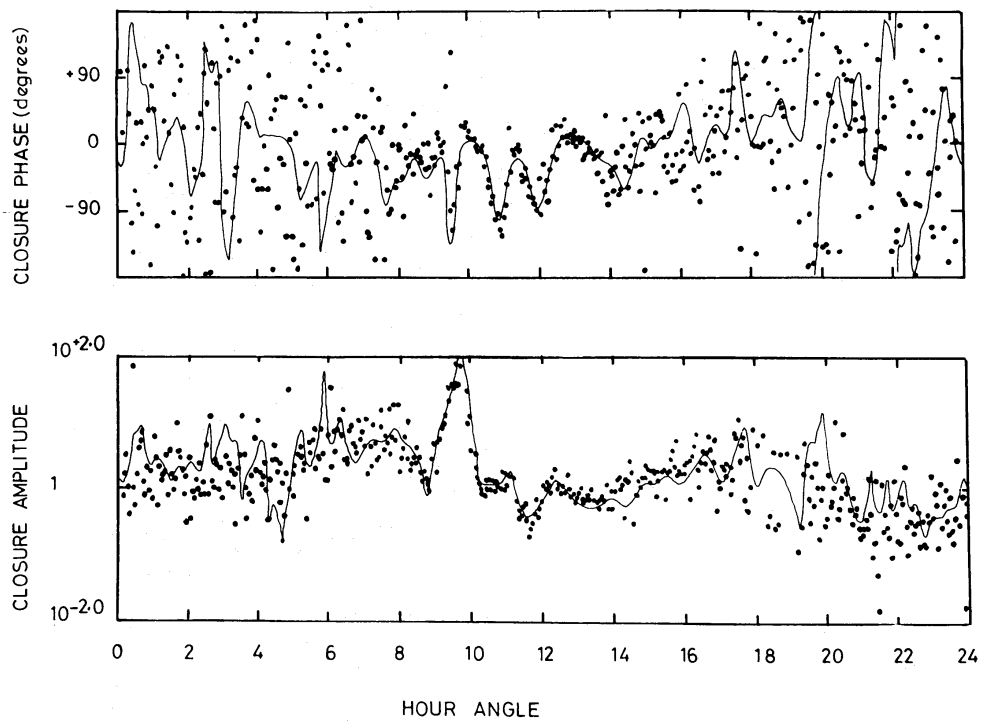

Figure 7. The fit to two of the closure quantities for the delta functions which are the basis of the hybrid map of Fig. 6. These are the equivalent of those shown in Fig. 5.

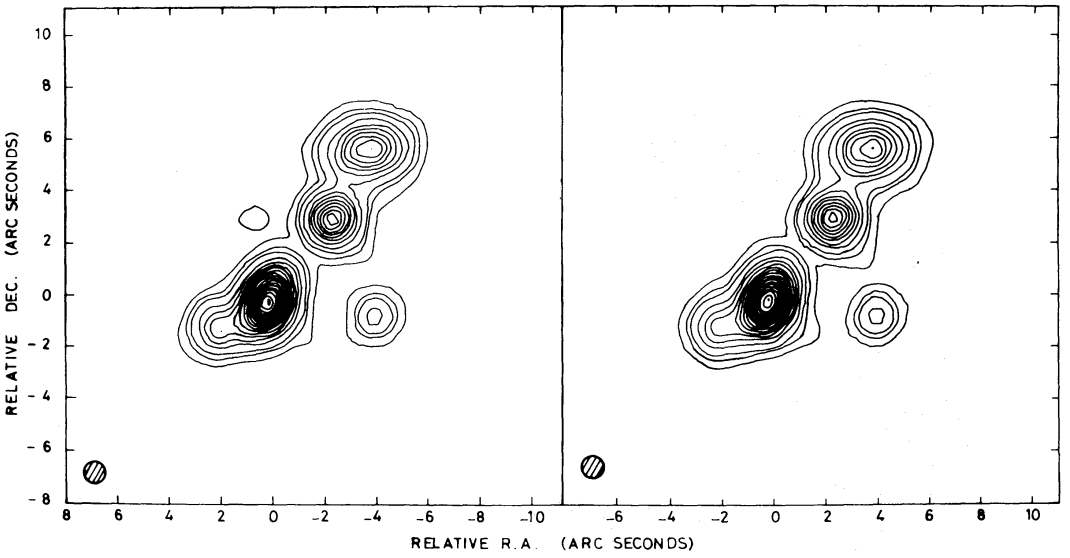

Figure 8. Test 4. The strong source with different levels of amplitude and phase stability at each telescope. (a) (left) A hybrid map made assuming no knowledge of the levels of errors at each telescope. The contour levels are 1, 3, 5, 10, . . . , 95 per cent. (b) (right) A hybrid map made assuming such knowledge. The contour levels are 1, 3, 5, 10, . . . , 95 per cent. A 1 per cent contour corresponds to 50 ± ~ 1 mJy per clean beam area.

the hybrid map is now 5 per cent of the peak brightness, while in the amplitude and phase-stable map it is still 1 per cent.

Test 3. Tests 1 and 2 have not been of the general case where there are different degrees of amplitude and phase stability at each telescope. For this final test we therefore constructed a data set where the phase stability (σ_{ϕ_j}) was approximately proportional to baseline length. On the shortest baseline it was 36° rms and it corresponded to complete phase instability on the longer baselines. The amplitude errors ranged from 1 to 15 per cent rms per telescope. We analysed these data in two ways: (1) assuming no knowledge of the relative errors on each telescope, and (2) assuming that the levels of these relative errors are known *a priori*; the first case corresponds closely to Schwab's assumptions.

In Figs 8(a) and (b) we show the final hybrid maps made under each assumption and using exactly the same number of iterations. It is clear that both the maps are slightly better than the earlier ones because we have added, on average, smaller errors. It is also clear that the inclusion of *a priori* information about the relative errors at each telescope enables us to make a better map. In this case, designed to simulate MTRLI observations, the differences are minor, but one can envisage situations where these differences would be considerably greater.

We summarize the results of these tests as follows.

(1) CORTEL enables us to make reliable hybrid maps from interferometer networks which have poor amplitude-stability and which are completely phase-unstable. Significant intervention by the user is not required to achieve convergence, notably because a point source is almost always adequate as the initial trial map. Typically 20 iterations were required to attain convergence starting from a point source.

(2) *A priori* estimates of the particular levels of amplitude and phase instability at each telescope, which are often available, are useful as extra constraints on the maps.

(3) The hybrid maps demonstrate that there is a loss in dynamic range compared with what would be obtained from a perfectly stable system, even when the signal-to-noise ratio is good. This is to be expected, since the closure quantities do not constrain the map as

strongly as do the true amplitudes and phases. For example, in the five-telescope MTRLI network there are 10 true amplitudes and 10 true phases for each integration period, whereas there are only five independent closure amplitudes and six independent closure phases. The loss in dynamic range is particularly severe if the signal-to-noise ratio on some baselines is poor. In such cases the effect of receiver noise is twofold. In addition to the degradation of the measurements of the individual amplitudes and phases, the estimates of the telescope errors, *used to correct data on other baselines,* are also unavoidably corrupted. In other words, high-quality closure information is only available if the signal-to-noise ratios of *all* the baselines in a loop are good.

(4) The five-telescope MTRLI can be used to make maps of the stronger complex sources reliable at the 2 per cent level or better. In our tests we have been pessimistic in our error assumptions, particularly as to the levels of amplitude instability to be expected. Also, at λ6 cm we anticipate that partial phase-stability may be achieved, at least on the shorter baselines, without phase-referencing. Even if phase-referencing on an unresolved source (Peckham 1973) is employed, CORTEL is still useful for further improving the map. This technique has been used by Noble & Walsh (1980) to map the DQSO 0957 + 56 at 408 MHz. Thus in many cases we expect that results intermediate in quality between these hybrid maps and the maps made from perfect stable data would be achieved. At λ73 and λ18 cm, the MTRLI will be operated as a six-telescope system. In this case there will not only be 50 per cent more amplitude and phase information but also twice as much closure information than we have used in these tests.

5 An MTRLI map of 3C 309.1 at 1666 MHz

A description of the MTRLI and its basic mode of operation has been given by Davies, Anderson & Morrison (1980). Since, for the present at least, nearly all the maps from this instrument will be produced using the technique we have just described, it is important to demonstrate in detail how we have analysed the data from an actual source.

The first observing session of the MTRLI in which five telescopes were employed was in 1980 August–September at 1666 MHz; observations of the quasar 3C 309.1 were made on August 13–14 and this high-declination ($\delta = 72^\circ$) source was tracked for almost a whole 24-hr period. The fringe amplitudes were calibrated, *baseline by baseline,* assuming that BL Lac was unresolved and had a flux density at the observing epoch of 5.95 Jy on the Baars *et al.* (1977) scale. This approach automatically corrects for the constant closure-amplitude errors of several per cent, very noticeable on BL Lac, believed to be caused by non-matched defining passbands. The gain stability of the system was such that we are confident of the individual fringe amplitudes to $\lesssim 2$ per cent rms. No attempt was made to calibrate the absolute phase of the interferometers. Constant offsets in the closure phases of up to 8°, whose exact origin is not known, were removed by an *ad hoc* procedure of adjusting the phases on six arbitrarily chosen baselines. In this way the closure phases were brought to zero, to better than 1°, on several calibration sources. Removal of the closure errors by this baseline-orientated calibration strategy noticeably improves the quality of the final map below the level of 1 per cent of the peak brightness.

The final hybrid map of 3C 309.1 derived from these data is shown in Fig. 9. No 'windows' were used in the CLEAN process to exclude possibly spurious regions of low brightness away from the main body of the source. The restoring beam is a circular Gaussian whose FWHM is 0.25 arcsec. In making this map we assumed that, except for MkII (see below), the amplitude error (σ_{a_j}) was ~2 per cent rms per telescope, while the phase errors (σ_{ϕ_j}) were assumed to be randomly distributed between ±180°. The receiver noise errors (σ_{jk}) were ~100 mJy rms in an integration time of 1 min on all baselines. In Fig. 10(a) and

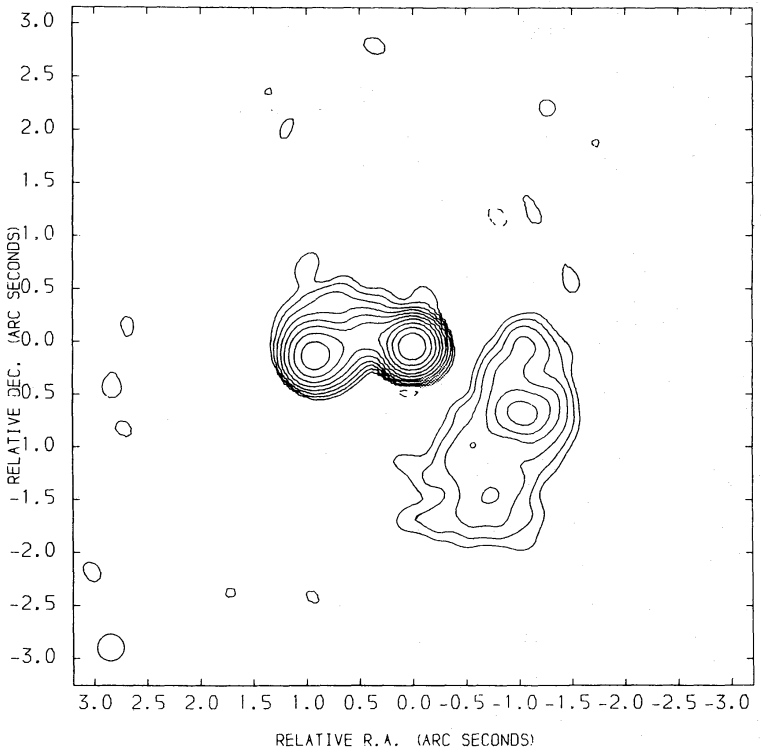

Figure 9. A hybrid map of 3C 309.1 made with five telescopes of the MTRLI at 1666 MHz. The contour levels are at 0.1, 0.2, 0.4, 0.8, 1.6, 3.2, 6.4, 12.8, 25.6, 51.2 per cent of the peak brightness. A contour level of 0.1 per cent corresponds to 3.8 mJy/beam area. The restoring beam is Gaussian of FWHM 0.25 arcsec.

(b) we show the fits to the observed closure phase and amplitude data of the Fourier transform of the point sources which are the basis of Fig. 9. In Fig. 10(c) we show the fits to the visibility amplitudes on the ten baselines. All maps made with the MTRLI and the CORTEL package are checked in this manner against the visibility data; in future, however, it is not intended to publish these data with each map.

In Table 1 we list the values of the mean and rms amplitude error assigned by CORTEL to each telescope. The mean errors reflect mistakes in the overall calibrations, while the rms errors are probably dominated by pointing inaccuracies. The peak discrepancies in the absolute amplitude fits are ~ 3 per cent and are most evident in the baselines involving the

Table 1. Values of the amplitude errors assigned by CORTEL to each telescope.

	II	Tabley	III	Knockin	Defford
Mean amplitude error (per cent)	0.0*	1.2	−0.6	0.2	0.0
Rms amplitude error (per cent)	0.0*	1.2	1.1	0.8	0.7

*Arbitrarily fixed to zero

Figure 10. (a) The fit to six independent closure-phases for the delta functions which are the basis of Fig. 9. The nomenclature TAB–DEF–III means $\theta_{\mathrm{TAB-DEF}} + \theta_{\mathrm{DEF-III}} + \theta_{\mathrm{III-TAB}}$; H.A. is hour angle in hours. In this, and in (b) and (c), the telescopes are identified as follows: II is the 37 × 25 m at Jodrell Bank, TAB and KNO are the 25-m VLA-types at Tabley and Knockin, III is the 37 × 25 m at Wardle, and DEF is the 25 m at Defford. Their locations are given in the paper by Davies, Anderson & Morison (1980). (b) The fit to five independent closure-amplitudes. The nomenclature is self-explanatory. (c) The fit to the 10 visibility-amplitudes.

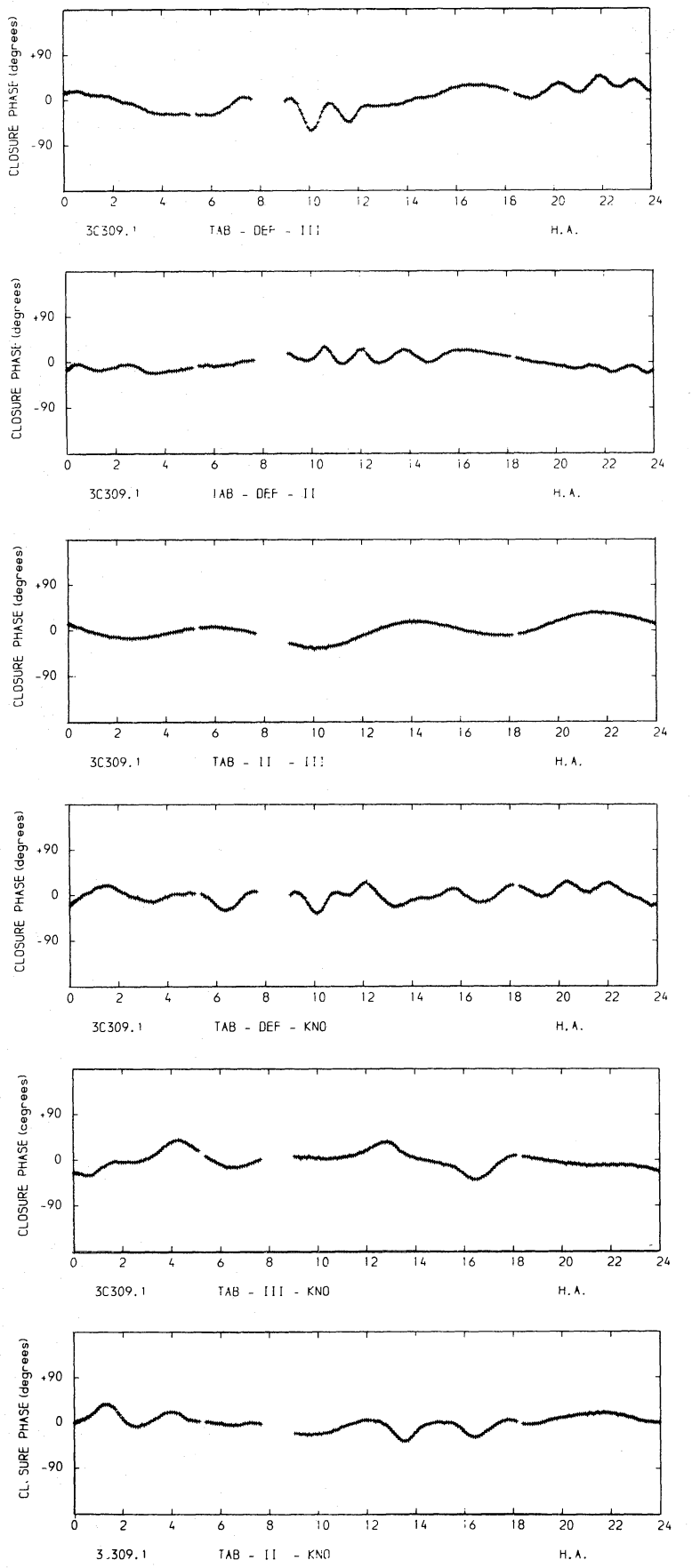

Figure 10 (a)

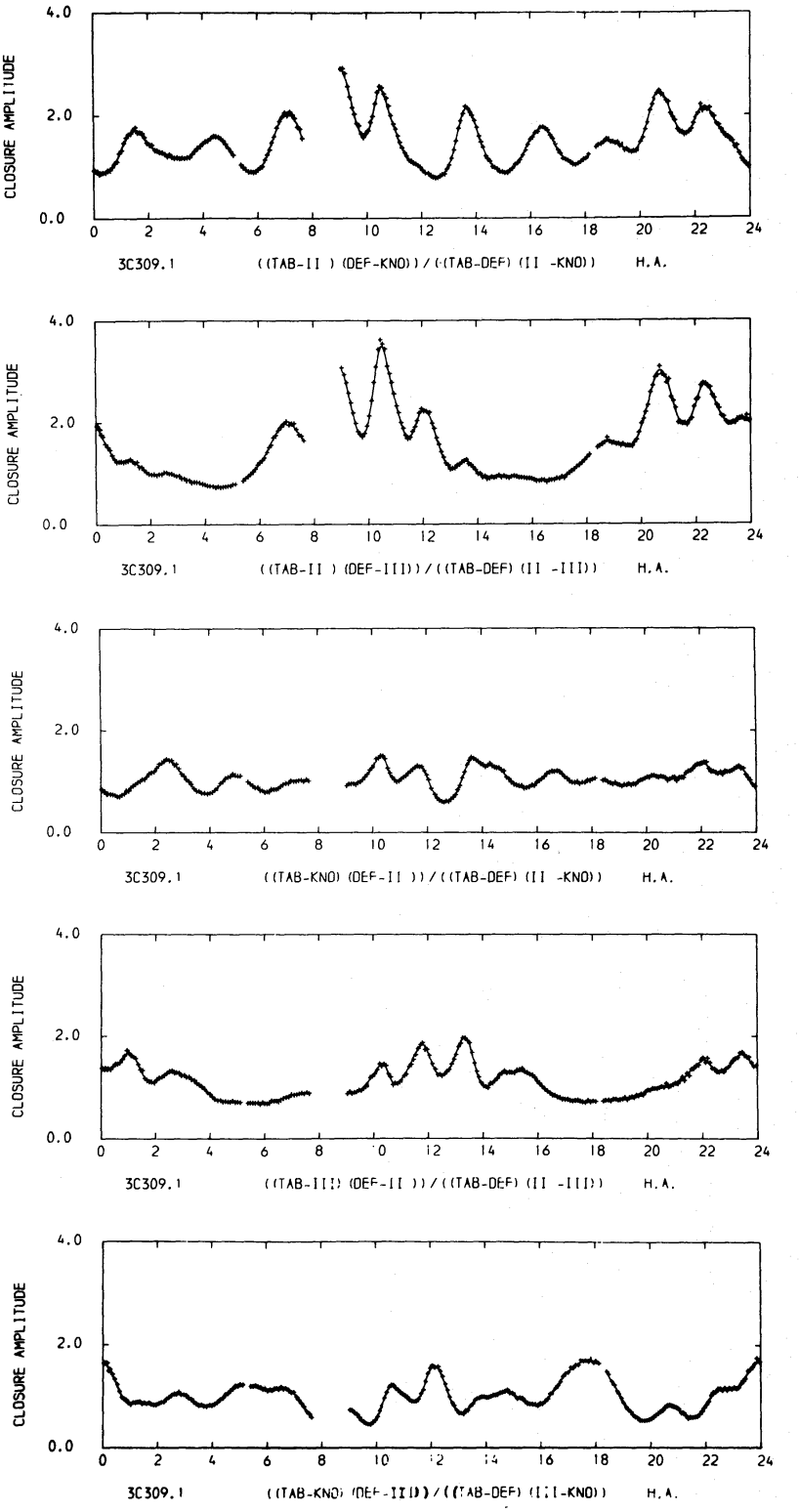

Figure 10 (b)

Tabley telescope, whose original calibration must have been systematically high by ~ 1 per cent. The flux density in the map, 6.9 ± 0.15 Jy, essentially accounts for the total flux density from the source. The uncertainty arises from the fact that the primary calibrator, BL Lac, was varying throughout the observing session and, while the baseline-to-baseline normalization is good to $\lesssim 1$ per cent, the absolute flux density scale is uncertain to ~ 2 per cent.

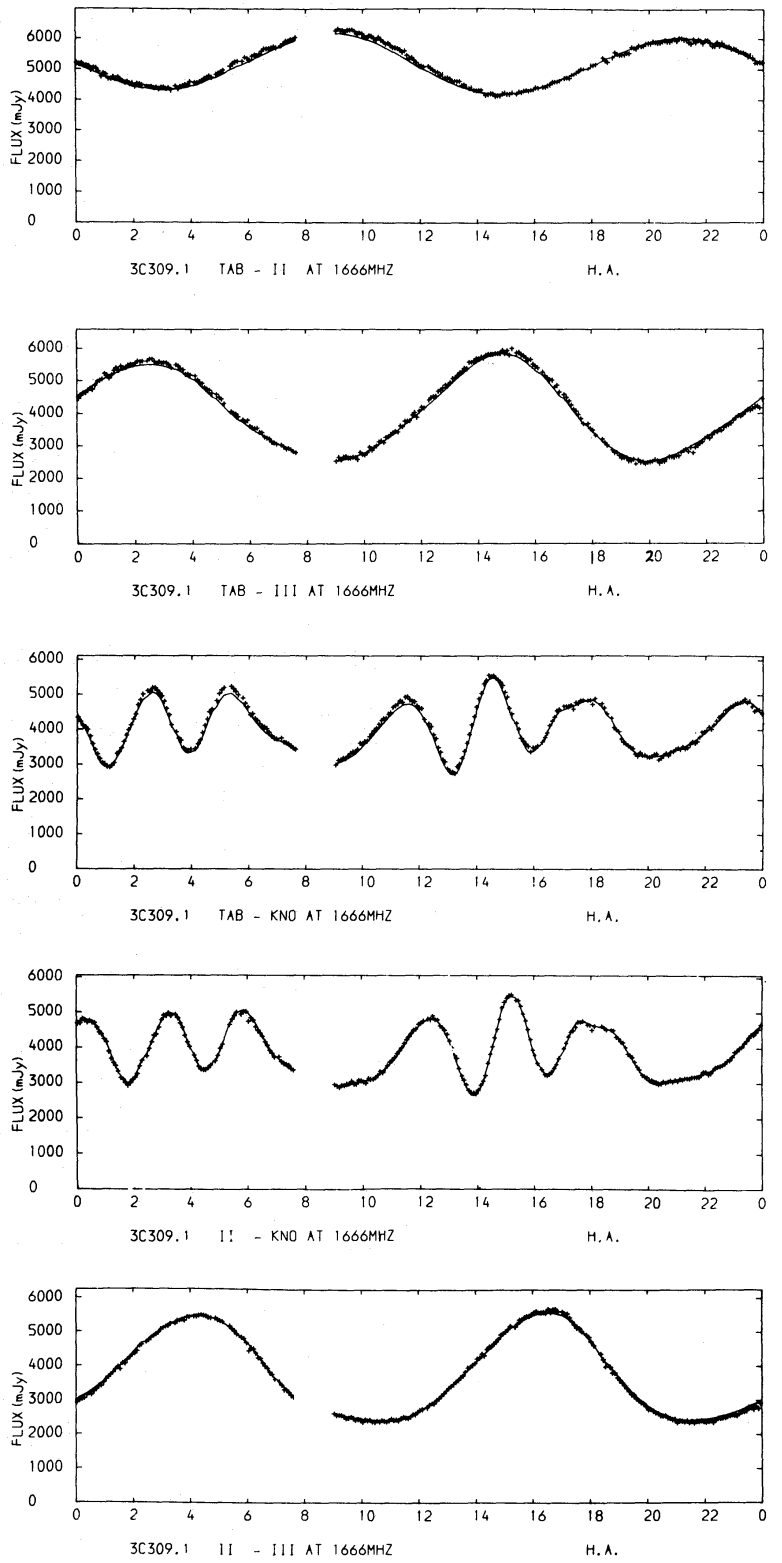

Figure 10 (c)

The lowest contour level on the hybrid map of 3C 309.1, 0.1 per cent of the peak brightness, i.e. a dynamic range of $\lesssim 1000{:}1$, is considerably better than that achieved in the tests described in Section 4. We can ascribe this improvement to a number of factors: (i) The structure of 3C 309.1 is relatively simple, and in particular has a central point-source producing ~ 50 per cent of the total flux density. This ensures that the signal-to-noise ratio is

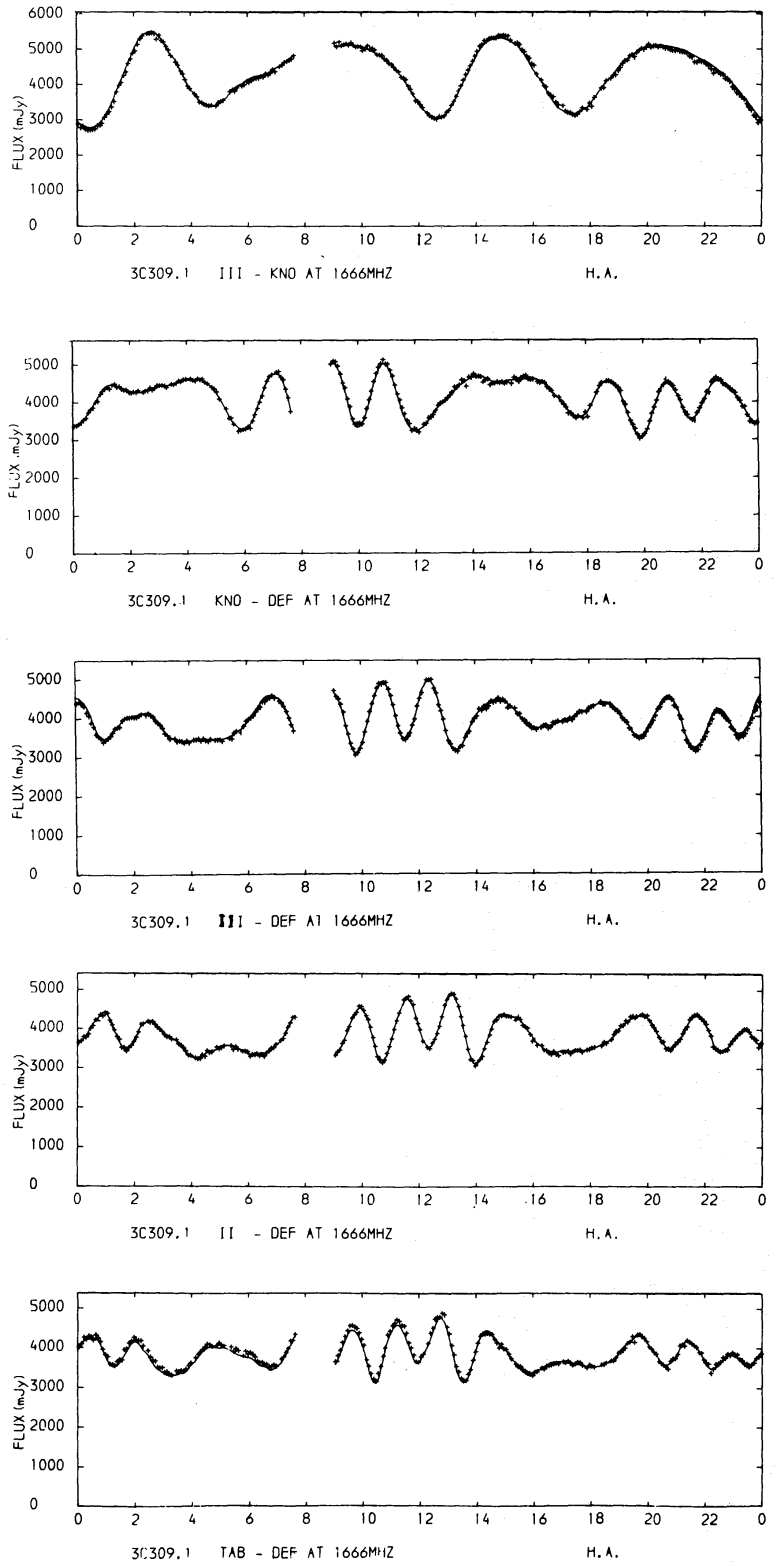

Figure 10 (c)

very high on all baselines at all times. (ii) The quality of the data is significantly better than assumed for the simulations. (iii) In the tests we usually allowed both the gain and the phase to vary as they pleased at each iteration. This is tantamount to mapping with only the five independent closure amplitudes and six closure phases. When the visibility amplitudes are as reliable as they are here, there is no need to allow the telescope gains to vary, except for a

few iterations at the end. Thus we have mapped this source principally using the 10 absolute amplitudes and the closure phases. This strategy improves the map by about a factor of 3 over that used in the tests, below the ½ per cent level of the peak brightness.

The lowest contour level plotted in the map corresponds to 3.8 mJy per beam, compared with the theoretical 2σ noise level for a perfectly amplitude- and phase-stable system of ~ 1.8 mJy per beam. It is clear then that, in a few nearly optimum cases such as this, one can approach the ideal CLEAN map using closure techniques. Of course, as the source of interest becomes weaker and/or more extended, it becomes considerably less likely that results comparable to the ideal will be obtained using only closure data.

Further discussion of this map of 3C 309.1 is deferred to a later paper.

6 Conclusion

We have developed and demonstrated the effectiveness of a new method of correcting data from partially stable interferometers which have been corrupted by errors attributable to individual telescopes in a network. It is equivalent to making explicit use of the closure phases and closure amplitudes as in several earlier algorithms. Our telescope-related method has advantages over earlier baseline-related methods; advantages which become significant when dealing with data from networks which have any of the following characteristics: (i) they consist of large numbers of telescopes, (ii) these telescopes have different degrees of amplitude and phase stability, (iii) the signal-to-noise ratio on some of the individual baselines is not high. No mathematical proof of convergence is presented (even if it were possible); our tests and extensive use at Jodrell Bank have nevertheless shown that, even when the visibility phases are highly perturbed, the method will converge from a very simple starting model, a point source often sufficing. Since the basic philosophy underlying our approach is similar to that of Schwab (1980), we would expect that the ultimate performances of the two methods would often be comparable. However, our method has simplifications and generalisations compared with Schwab's which make it more suitable for analysing MTRLI data which are less homogeneous and less phase-stable than the data from the VLA.

The reliability of this hybrid-mapping procedure is such that one can have confidence in the maps produced by the MRTLI, or indeed any multi-telescope network, even if the absolute fringe amplitudes and phases are unobtainable.

Acknowledgments

We thank Roger Noble and Mike Charlesworth for their computing efforts which made the running of these programs so much easier, and Andrejz Kus for the initial analysis of the 3C 309.1 map. We are also grateful to John Ponsonby, Ian Morison and Ron Clark for their comments on an earlier version of this paper which enabled it to be significantly improved. TJC acknowledges the receipt of an SRC Postdoctoral Fellowship and PNW acknowledges the receipt of the Royal Society Weir Fellowship during the period of this work.

References

Baars, J. W. M., Genzel, R., Pauliny-Toth, I. I. K. & Witzel, A., 1977. *Astr. Astrophys.*, **61**, 99.
Baldwin, J. E. & Warner, P. J., 1976. *Mon. Not. R. astr. Soc.*, **175**, 345.
Cotton, W. D., 1979. *Astr. J.*, **84**, 1122.
Davies, J. G., Anderson, B. & Morison, I., 1980. *Nature*, **288**, 64.
Fomalont, E. B., 1973. *Proc. I.E.E.E.*, **61**, 1211.
Fort, D. N. & Yee, H. K. C., 1976. *Astr. Astrophys.*, **50**, 19.
Högbom, J. A., 1974. *Astr. Astrophys. Suppl.*, **15**, 417.

Jennison, R. C., 1953. *PhD Thesis,* Victoria University of Manchester.
Jennison, R. C., 1958. *Mon. Not. R. astr. Soc.,* **118,** 276.
Noble, R. G. & Walsh, D., 1980. *Nature,* **288,** 69.
Peckham, R. J., 1973. *Mon. Not. R. astr. Soc.,* **165,** 25.
Readhead, A. C. S. & Wilkinson, P. N., 1978. *Astrophys. J.,* **223,** 25.
Readhead, A. C. S., Walker, R. C., Pearson, T. J. & Cohen, M. H., 1980. *Nature,* **285,** 137.
Rogers, A. E. E. *et al.,* 1974. *Astrophys. J.,* **193,** 293.
Schwab, F. R., 1980. *Proc. 1980 Int. Optical Computing Conf.,* Soc. Photo-Optical Engineers, in press.
Thompson, A. R., 1980. *V.L.A. Electronics Memorandum No. 192.*
Twiss, R. W., Carter, A. W. L. & Little, A. G., 1960. *Observatory,* **80,** 153.